Hygrothermal ageing effects on mode I fatigue delamination in multidirectional composite laminates

Yao, Liaojun; He, Zixian; He, Yonglyu; Jin, Qifeng; Lomov, Stepan V.; Alderliesten, Rene C.

DOI
10.1016/j.ijfatigue.2024.108520

Publication date
2024

Document Version
Final published version

Published in
International Journal of Fatigue

International Journal of Fatigue 188 (2024) 108520

Contents lists available at ScienceDirect

International Journal of Fatigue

journal homepage: www.elsevier.com/locate/ijfatigue

Hygrothermal ageing effects on mode I fatigue delamination in multidirectional composite laminates

Liaojun Yao [a,*], Zixian He [a], Yonglyu He [b], Qifeng Jin [b], Stepan V. Lomov [c], Rene C. Alderliesten [d]

[a] Department of Astronautics Science and Mechanics, Harbin Institute of Technology, Harbin, PR China
[b] Department of Material Science and Engineering, National University of Defense Technology, Changsha, PR China
[c] Department of Materials Engineering, KU Leuven, Belgium
[d] Faculty of Aerospace Engineering, TU Delft, The Netherlands

ARTICLE INFO

Keywords:
Fatigue
Delamination
Environmental ageing
Damage mechanism
Composite laminates

ABSTRACT

Ageing is known to have significantly detrimental effect on mode I fatigue delamination growth (FDG) in unidirectional (UD) composite laminates. However, composite structures are usually designed with multidirectional (MD) layups, which raises the question that is it enough to only conducted fatigue delamination experiments on specimens with a UD layup. The aim of this study is therefore to explore mode I FDG in MD composite laminates with 45//45 interface after different ageing, i.e. at 70 °C 85 % relative humidity (RH) and immersion in 70 °C water bath. Fatigue delamination experiments were conducted at stress ratios $R = 0.1$ and 0.5. The fatigue data, interpreted via Paris-type fatigue laws, demonstrated that: (1) the change of ageing severity has no influence on mode I FDG in MD composite laminates; (2) FDG remains the same in composite laminates after different ageing, regardless of layups. In all cases, the same master resistance curves can be obtained to determine the intrinsic mode I fatigue delamination resistance of UD and MD composite laminates after different ageing. The physical reasons for these findings were discussed based on the moisture content analysis, Fourier transform infrared (FTIR) analysis, dynamic mechanical thermal analysis (DMTA), and fractographic examinations. It was found that material degradation and delamination mechanisms remain the same for UD and MD layups, as well as for 85 %RH and water bath conditioning.

1. Introduction

Fatigue delamination growth (FDG) is one of the most important failure modes frequently reported in aeronautical composite structures in their long-term service life [1,2], as has been established in the design practice by the introduction of slow crack growth philosophy in composite structure certification by US federal aviation administration (FAA) Advisor Circular AC 20-107B since 2009 [3]. The initiation and propagation of this damage can have significantly detrimental effects on the integrity of a composite structure, thus making it crucial to have in-depth understanding on this phenomenon. In the past several decades, both European Structural Integrity Society Technical Committee 4 (ESIS TC4) and ASTM D30 have performed separated round-robin test programs to develop a test protocol for characterizing mode I FDG in composite laminates [4–8].

Fatigue delamination is essentially a material fracture phenomenon. Fracture mechanics have been widely used in fatigue delamination representation of composite laminates, based on the success of these methods in fatigue crack characterization for metals [9,10]. Particularly, fatigue delamination is usually correlated to the strain energy release rate (*SERR*) G, instead of the stress intensity factor (*SIF*) K, for the heterogeneous of composite materials. However, there is no consensus on the specific formulation of *SERR* in FDG determination, which enters the Paris-type relations for crack growth [9–11]. Some scholars used the maximum *SERR* $G_{\max}$ or the *SERR* range $\Delta\sqrt{G}$ in FDG characterization [11,12,4,5], whereas others recommended to employ both $G_{\max}$ and $\Delta\sqrt{G}$ with the perspective of full fatigue load description [13]. The key point in the choice of the *SERR* formulation is similitude [14]. Inconsistency in the similitude parameters can result in different conclusions in FDG interpretation. Taking R-ratio dependence as a typical example, there are both reports on decrease [15] or increase [16], or even no obvious influence [17–19] of fatigue delamination with stress ratio. As a result, it is important to employ the Paris-type relations with appropriate *SERR* formulations well representing similitude in FDG characterization.

* Corresponding author.
E-mail address: L.Yao@hit.edu.cn (L. Yao).

https://doi.org/10.1016/j.ijfatigue.2024.108520
Received 25 April 2024; Received in revised form 2 July 2024; Accepted 20 July 2024
Available online 22 July 2024

The majority of the above mentioned studies were carried out on specimens with UD layup, hence 0//0 configuration of the interface. However, aeronautical composite structures are usually designed with MD layups, rather than only UD layup that recommended in the standard test used by the research community. Referring to quasi-static studies [20–22], the difference in layups, such as from UD to MD, may have important effects on damage mechanisms (such as crack migration, zig-zag crack propagation, or more or less fibre bridging development), finally contributing to delamination resistance. All these mechanisms can affect fatigue delamination resistance of a composite material. Limited work exists [23–30] with MD layup fatigue delamination, and only few studies [23–25] were performed to make a comparison on FDG between MD and UD composite laminates. To the best knowledge of the authors, this comparison still stays controversial. In [23], it was reported that fatigue delamination threshold of MD composite laminates is much higher than that of UD, for more fibre bridging generation. In work [24], the fastest fatigue crack growth rate was observed in UD case as compared to MD layups. A different phenomenon is reported in [25] that the change in interface configuration had negligible effect on mode I fatigue delamination threshold.

Composite structures can endure different hygrothermal exposure in their long-term operation. Moisture diffusion in composite laminates can induce mechanical deterioration in both matrix and fibre/matrix interface, and even cause micro/macro damage evolution such as cracking/debonding or pores/voids generation [31–33]. It has been reported that environmental ageing can have significant effects on mode I delamination resistance of composite materials, as well as the damage mechanisms under quasi-static or fatigue loading [34–38]. There is a controversy on ageing effects on fatigue delamination resistance in composite laminates. It was reported that environmental ageing can decrease FDG because of matrix or bond ductility increase [39,40]. In another study [41], it was found that hygrothermal ageing can promote faster crack propagation for interface degradation. In spite of the controversy in literature [39–41], our previous work [38] has clearly demonstrated that environmental ageing can increase FDG rate by a factor of ~ 5. These detrimental effects induced by water absorption can make the layup dependence or independence of FDG behaviour even more complicated.

In addition to damage evolution concentrated around the crack front, fibre bridging is an important shielding mechanism frequently reported in mode I fatigue delamination of composite laminates [6,8,12,23,27]. How to appropriately interpret mode I fatigue delamination with large-scale fibre bridging is in the centre of ISO standardization, aimed by ESIS TC4 and ISO/TC61/SC13 [8,42]. There is solid evidence that both layups [21,22] and long-term environmental exposure [36,43] can affect the fibre bridging. The change of stacking sequence from UD to MD usually promotes more fibre bridging in quasi-static delamination, due to the presence of intralaminar damage or zig-zag crack propagation occurring in the neighbouring layers [20,22]. More bridging fibres can be present in fatigue delamination of aged composite laminates [38], because of fibre/matrix interface degradation. Similar conclusion was also made in [36,43]. Thus, it is important to have further investigation on mode I fatigue delamination with large-scale fibre bridging in MD composite laminates after environmental ageing.

According to above discussion and the authors' recent study [38], a subsequent investigation was conducted in the present work to answer the following questions:

1. What effects does ageing severity have on mode I fatigue delamination of MD composite laminates, and the corresponding damage mechanisms?
2. Is there layup dependence on mode I fatigue delamination in composite laminates after ageing with different severity?

The answers for these questions will be useful for composite structure design, especially with the introduction of low crack growth philosophy in the certification that recommended by the FAA. Furthermore, this study can provide extra evidence on the validation of both the test program and the data reduction models for ISO mode I fatigue delamination test standard development of composite laminates that aimed by ESIS TC4 and ISO/TC61/SC13.

Mode I fatigue delamination experiments were carried out on double cantilever beam (DCB) specimens with MD layup, 45//45 interface, after different ageing conditions, 70 °C 85 % RH and 70 °C water bath (WB). All fatigue delamination data were interpreted via two Paris-type laws. Both FTIR and DMAT analysis were performed to have relevant information on material degradation induced by water absorption. Fractographic examinations were carried out to explore the material degradation and fatigue delamination mechanisms of MD composite laminates after different environmental ageing.

2. Materials, experimental setup and methodology

2.1. Specimen manufacturing and conditioning

DCB specimens were manufactured using prepreg of UD continuous carbon fibres in a thermosetting epoxy matrix, M30SC/DT120, supplied by Delta-Tech S.p.A, Italy (see Appendix for detailed information of this prepreg). In accordance with our previous studies [23,27], MD composite laminates were design with a layup $[(\pm45/0_{12}/\mp45)//(\pm45/0_{12}/\mp45)]$ to avoid crack jumping, and minimize both residual thermal stress and non-uniform energy release rate distribution across the width of the crack front [20,44]. A schematic diagram of the layup is illustrated in Fig. 1. A 12.7 μm Teflon film was inserted into the mid-plane of the composite panel at one end to introduce an initial delamination, typically around $a_0 = 60$ mm. These laminates were cured in autoclave at a pressure of 6 bar and a temperature 120 °C for 90 min, as recommended by the supplier. After curing, composite laminates with a nominal thickness of 5 mm were C-scanned to guarantee there is no obvious manufacturing imperfection. The MD DCB specimens 200 mm × 25 mm were cut from these panels with the long direction aligned with the 0° fibre direction, according to the ASTM D5528 standard [45].

A pair of aluminium loading blocks, 25 mm width by 20 mm length with 6 mm thickness, was adhesively bonded on the DCB specimens at the side of Teflon insert for introducing cyclic loads. One side of each DCB specimen was coated with a thin layer of typewriter correction fluid to enhance the visibility of delamination front during the fatigue test. A strip of grid paper was pasted on this coated side to aid in measuring crack propagation length.

DCB specimens with 45//45 interface were conditioned at two typical environments, i.e. 70 °C 85 % RH and 70 °C WB, using the WEISS WK111-340 environmental chamber, according to the ASTM D5229 standard [46]. The weights of three conditioned samples for each environmental ageing were measured with pre-defined time intervals until moisture absorption equilibrium, i.e. the state that the effective moisture equilibrium changes less than 0.02 % within the reference time span. This definition of the equilibrium is given by ASTM D5229 standard, and used in literature, for example [47]. This finally results in the total exposure time of four months for WB specimens and almost six months for 85 %RH ones. These measured mass data enable moisture content M calculation, which was subsequently analyzed via the Fickian diffusion law following the standard [46]. All these conditioned MD DCB specimens at moisture equilibrium were appropriately stored in the environmental chamber until the moment of the fatigue tests at the ambient conditions, i.e. at temperature 20-25 °C 50 %RH.

2.2. Fatigue delamination experiments and data reduction methodology

All mode I fatigue delamination experiments were conducted on a 15 kN MTS hydraulic-servo test machine at a relative low frequency 5 Hz (avoid heating effects) with stress ratios $R = 0.1$ and 0.5 under displacement control, according to the specific test protocol proposed in

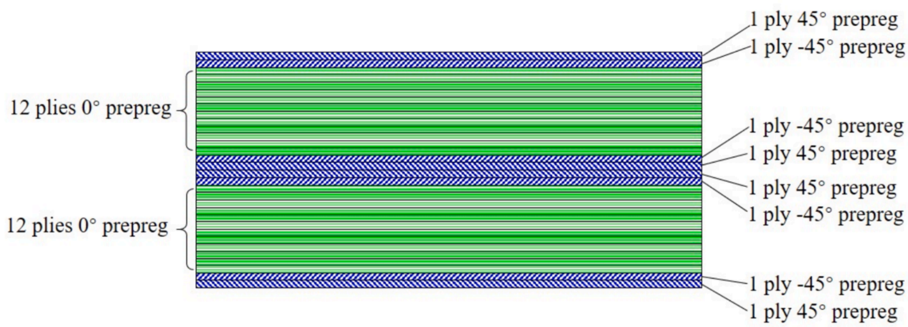

Fig. 1. A schematic illustration of the MD layup.

the previous studies [23,27,38,42]. A schematic illustration of this specific test procedure has been provided in [48], see Fig. 2(a). With this test procedure, multiple fatigue delamination tests could be performed on the same DCB specimens at a given *R*-ratio, but with a succession of fatigue pre-crack lengths. The different initial crack lengths lead to different amounts of fibre bridging. Multiple fatigue delamination resistance curves, with each one representing FDG with a certain amount of fibre bridging, and the fatigue R-curve $G_{IC}(a\text{-}a_0)$, representing interlaminar resistance increase because of fibre bridging, can be obtained.

Similar to what has been reported in [49] using video image processing in determining fatigue delamination length during the test, a computer controlled digital camera system with high resolution was used to monitor delamination propagation length during the experiments in the present study. According to this system, images of the fatigue crack extension at one side of the specimen were automatically recorded at the maximum displacement during the test with pre-defined intervals. Particularly, the interval was set to be every 100 cycles in the first 5000 fatigue cycles, every 500 cycles in the following 15,000 fatigue cycles, and every 1000 cycles when the fatigue cycle number exceeds 20000. These recorded images were analysed after the tests via ImageJ software to measure crack propagation lengths at different fatigue cycles. This experimental setup is illustrated in Fig. 2(b). Table 1 summarizes all fatigue delamination experiments with different fatigue pre-crack lengths (i.e. different amounts of fibre bridging).

The modified Paris law Eq. (1) [27] and the two-parameter fatigue model Eq. (2) [19] were employed to perform the data reduction. This allows determining the intrinsic fatigue delamination resistance around the crack front excluding fibre bridging. The use of the two-parameter model is to account for *R*-ratio effects in intrinsic fatigue delamination resistance characterization.

$$\frac{da}{dN} = C\Delta G_{tip}^{n} = C\left[\frac{G_{IC0}}{G_{IC}(a-a_0)}\left(\sqrt{G_{\max}} - \sqrt{G_{\min}}\right)^2\right]^n \tag{1}$$

$$\frac{da}{dN} = C\Delta G_{eff}^{n} = C\left[\Delta G_{tip}^{\left[1-\left(\frac{G_{\max\_tip}}{G_{IC0}}\right)^{\gamma}\right]} G_{\max\_tip}^{\left(\frac{G_{\max\_tip}}{G_{IC0}}\right)^{\gamma}}\right]^n \tag{2}$$

where C and n are curve-fitting parameters for the Paris-type correlations; $G_{\max}$ and $G_{\min}$ respectively represent the maximum and minimum *SERR* of a fatigue cycle, which can be determined via the modified compliance calibration method (MCC) Eq. (3) recommended in the ASTM D5528 standard [45]; $G_{\max\_tip}$ and ΔG_{tip} determine the maximum *SERR* and *SERR* range around the crack front; $G_{IC}(a\text{-}a_0)$ is the fatigue R-curve; G_{IC0} is fatigue resistance excluding fibre bridging, i.e. $G_{IC}(0)$; γ can be best interpreted as the weight-parameter; and da/dN is the fatigue crack growth rate, which can be determined via the seven-point incremental polynomial method recommended in the ASTM E647 standard [50].

$$G = \frac{3P^2C^{(2/3)}}{2A_1Bh} \tag{3}$$

where P is the load; C is the compliance of the DCB specimen; A_1 is the slope of the curve in the graph where a/h is plotted against $C^{1/3}$.

2.3. FTIR analysis

FTIR spectroscopy was employed to identify the changes of chemical bands and functional groups of composite material M30SC/DT120 before and after different environmental ageing. These samples were scanned via a Thermo Scientific Nicolet IS50 FTIR instrument at a resolution of 4 cm^{-1} in attenuated total reflection (ATR) to obtain the FTIR spectrum in the wavenumber range of 400 to 4000 cm^{-1} with 16 scans per spectrum.

2.4. DMTA experiments

DMTA experiments were conducted to have information of environmental aging effects on mechanical degradation of the composite material M30SC/DT120. These experiments were performed in PerkinElmer DMA8000 dynamic mechanical analyser via single cantilever beam with dimensions of 20 mm length by 5 mm width and thickness. All these experiments were conducted at a temperature range between 25 °C and 200 °C with a frequency of 1.0 Hz and temperature ramp rate of 5 °C/min.

2.5. SEM fractographic analysis

SEM observations on aged/un-aged material morphology and fatigue delamination surfaces were conducted on TESCAN AMBER GMH. The SEM samples were prepared with gold sputter-coating in vacuum to avoid static charging due to the non-conductive nature of the material used in the present study.

3. Results and discussions

A comparison based on the Fickian diffusion law was first carried out to have detailed information of ageing severity effects on moisture absorption in Section 3.1. Both FTIR and DMTA analysis were subsequently performed to provide necessary information of environmental ageing effects on material's chemical structure and glass transition temperature T_g in Sections 3.2 and 3.3. In Section 3.4, all fatigue data were interpreted via Eqs.(1) and (2) to explore ageing severity and layup effects on the intrinsic fatigue delamination resistance of MD composite laminates. In Section 4, fractographic analysis was conducted, supported by the FTIR and DMTA results, to identify the physical reasons for environmental ageing and layup effects on mode I fatigue delamination of MD and UD composite laminates.

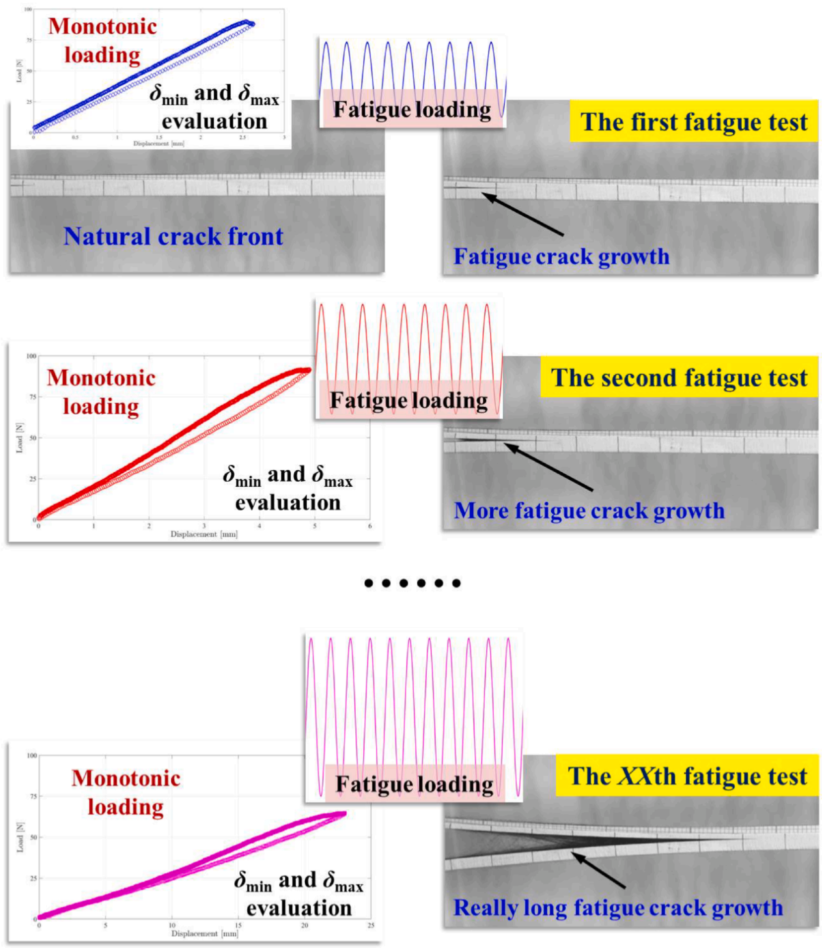

(a)

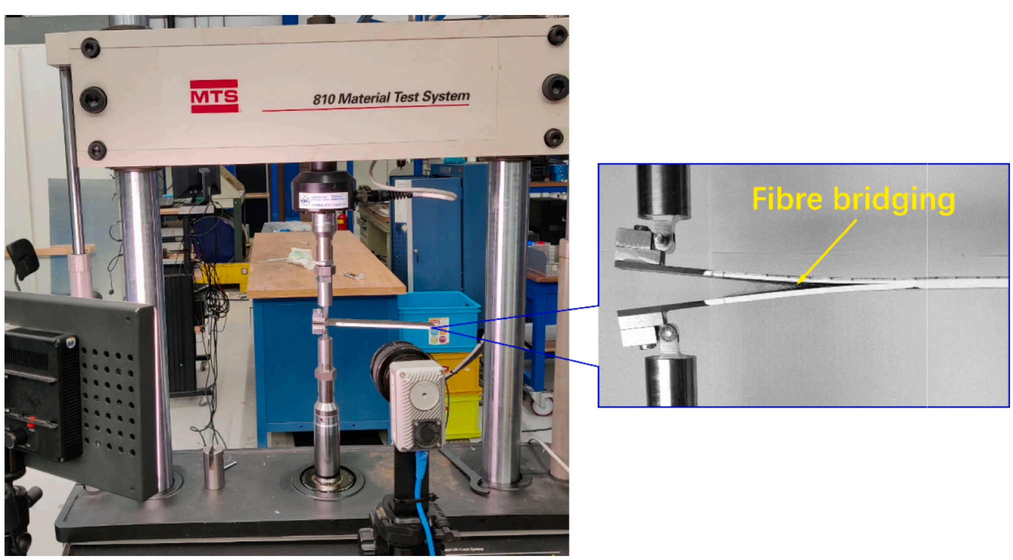

(b)

Fig. 2. Mode I fatigue delamination with fibre bridging: (a) A schematic illustration of the test procedure for fatigue delamination with fibre bridging [48]; (b) Fatigue experimental setup.

Table 1
Mode I fatigue delamination test matrix.

Sample	*R*-ratio	Fatigue pre-crack length *a*-a_0 [mm]
85 %RH-Spe-1	0.1	0.68; 11.04; 25.81; 43.17; 64.52
85 %RH-Spe-2	0.5	2.10; 11.21; 19.02; 27.73; 36.27; 47.35; 58.27
85 %RH-Spe-3		2.34; 9.96; 17.09; 25.86; 36.00; 47.03
WB-Spe-1	0.1	4.22; 17.77; 34.47; 54.32; 72.95
WB-Spe-2	0.5	5.36; 13.33; 21.95; 30.38; 41.43

3.1. Moisture absorption

Fig. 3 provides the moisture absorption curves, in terms of percent moisture content against immersion time, for MD composite laminates after different environmental ageing. The results demonstrate that ageing conditions have important influence on material's water immersion performance. The moisture content increases much faster and achieves a higher plateau (1.22 ± 0.02 %) with shorter exposure for WB condition, as compared to 85 %RH (0.72 ± 0.02 %). The Fickian diffusion law can well determine the moisture absorption behaviour of MD composite laminates at different ageing conditions.

Table 2 provides a summary of the equilibrium moisture contents for both UD and MD composite laminates after different ageing. UD and MD composite laminates have the same equilibrium moisture contents after the same environmental ageing.

3.2. Characteristic FTIR bands

The FTIR spectra of aged/un-aged MD and UD composite laminates is illustrated in Fig. 4, as an evidence to identify if there is any change in bonds and functional groups in the un-aged and aged composite material by analysing the peak intensity at different wavenumbers.

According to the infrared spectrum, it is evident that intensity changes were observed at wavenumbers 3300, 1640, 1606, 1580, and 1508 cm^{-1} for MD composite laminates as illustrated in Fig. 4(a), which corresponding to different groups and molecules shown in Table 3. Particularly, the broad peak at 3100 ~ 3600 cm^{-1} represents the O–H stretching and the intermolecular hydrogen bonds [52]. This peak is observed at 3300 cm^{-1} in the present study. In addition, the absorption intensity at 1640 cm^{-1} (corresponding to the carbonyl group C = O) was identified in composite material after environmental ageing. All these indicate that hygrothermal ageing can induce hydroxyl group formation with moisture immersion in the epoxy resin. The hygrothermal ageing can also increase the free water content in the carbon fibre reinforced epoxy composite, which can also lead to the intensity increase at 3300 cm^{-1}. In addition, the intensity increase at 1640 cm^{-1} (corresponding to

Table 2
Equilibrium moisture contents for UD and MD composite laminates.

	70 °C 85 %RH	70 °C WB
UD composite laminates**	0.74 ± 0.02 %	1.20 ± 0.02 %
MD composite laminates	0.72 ± 0.02 %	1.22 ± 0.02 %

** Data of UD composite laminates are from [38,51].

the carbonyl group C = O) indicates that hygrothermal ageing can cause hydrolysis reaction via attacking the polymer networks as

$$\mathrm{RCOOR'} + \mathrm{H_2}O \leftrightarrow \mathrm{RCOOH} + \mathrm{R'}OH \tag{4}$$

This reaction is reversible, which can be partial or full recovery after water desorption. The peaks at 1606, 1580, and 1508 cm^{-1} are related to the carbon–carbon double bond peaks on the benzene ring [53,56]. These chemical bonds of methylene and benzene were extremely stable for composites after ageing. As a result, these intensity decreases in spectrum band after hygrothermal exposure may be due to the increase in the material surface roughness or material homogeneity, leading to a decrease in the intensity of ATR testing during the process.

Fig. 4(b) provides the FTIR spectra of UD composite laminates. No obvious difference (i.e. the location of the peak) in the infrared spectrum was observed between UD and MD after environmental ageing. This means that the same or similar changes may occur in UD composite laminates after environmental ageing, as compared to MD composite laminates, which agrees well with the equilibrium moisture content information given in Table 2.

According to the FTIR analysis, it can be concluded that: (1) there is no evidence of obvious irreversible chemical change occurring during the hygrothermal ageing, and the main physical process occurring in the composite laminates may be matrix swelling caused by the infiltration of water molecules; (2) neither ageing severity nor layups has obvious effect on material chemical structure (change) after environmental ageing.

3.3. DMTA analysis

Fig. 5 provides the DMTA results in terms of damping factor tanδ against temperature T for un-aged and aged composite laminates with/without water desorption, which were used for glass transition temperature T_g definition via the peak of these curves. It is clear that environmental ageing and the followed drying treatment can have obvious effects on the shapes of the DMTA results, contributing to different values of T_g.

Table 4 gives a summary of T_g for MD and UD composite laminates after different environmental exposure. The results demonstrate that

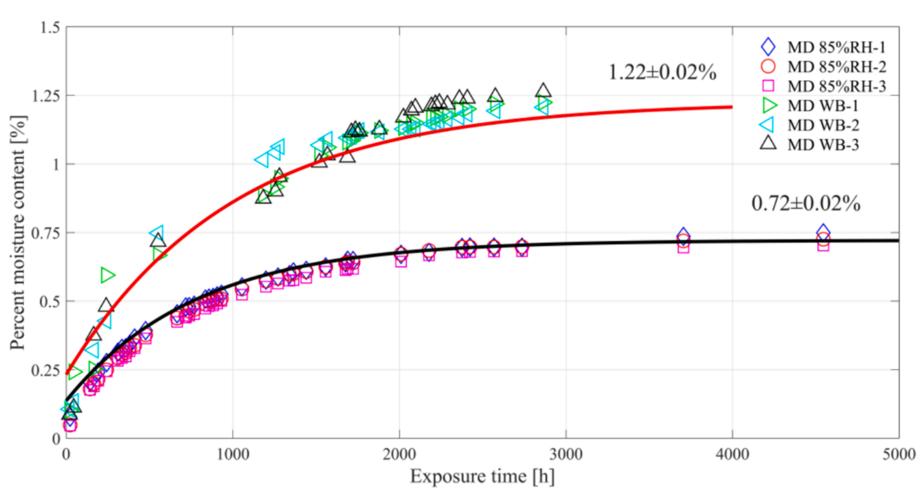

Fig. 3. Moisture absorption curves for MD composite laminates.

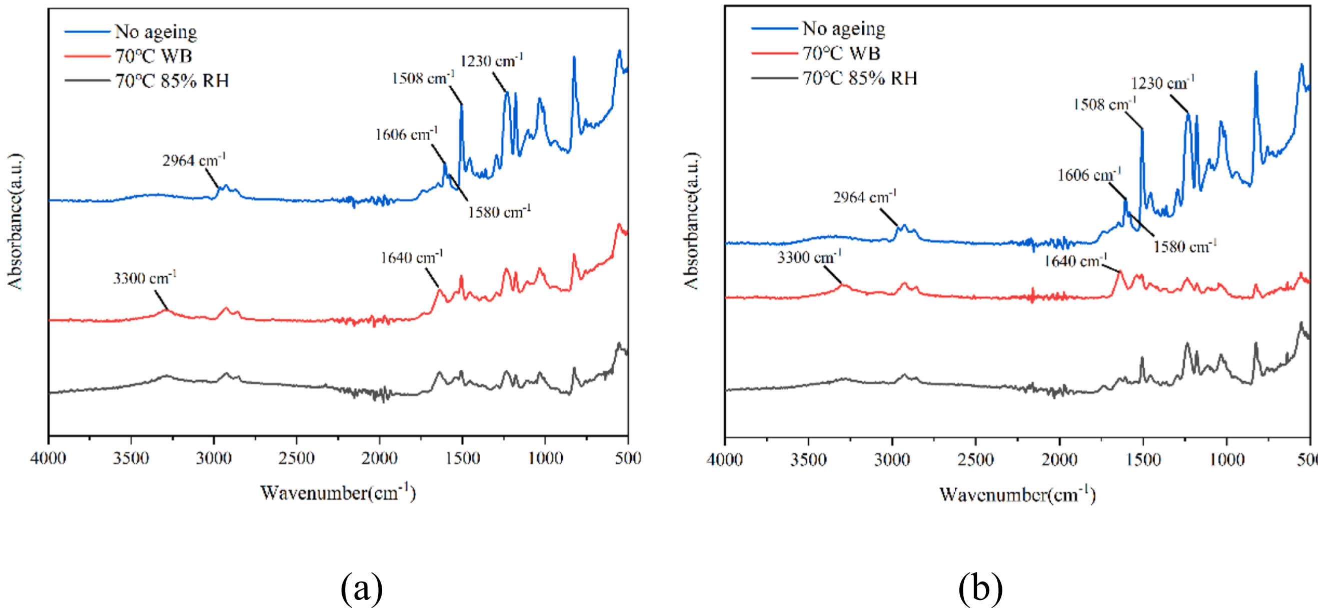

Fig. 4. Infrared spectrum analysis for composite laminates with/without ageing (a) MD composite laminates; (b) UD composite laminates.

Table 3
The major bands in FTIR spectrum of the epoxy resin [52–55].

Bands (cm^{-1})	Assignment
3300	Hydroxyl (–OH) stretching
1640	Carbonyl group (C = O)
1606, 1580,1508	Stretching of the benzene ring

hygrothermal ageing can cause obvious degradation of MD composite laminates, as indicated by the decrease of T_g. Particularly, the magnitude of T_g decreases from 133.0 °C to 106.3 °C for 85 %RH, and to an even lower 95.6 °C for WB. Partial recovery is observed in aged composite material after drying treatment. It is interesting that the difference in T_g for different ageing conditions (i.e. 85 %RH and WB) becomes narrow (i.e. 109.3 °C vs. 105.5 °C) after drying, as compared to the initial condition without drying (i.e. 106.3 °C vs. 95.6 °C). This finding is the same as what has been reported in UD composite laminates in [38,51].

Furthermore, the magnitude of T_g for UD and MD composite laminates is similar after a given environmental ageing without drying (107.4 °C vs. 106.3 °C 85 %RH, 96.5 °C vs. 95.6 °C WB). After drying, these conditioned UD and MD composite laminates still have the similar T_g (111.5 °C vs. 109.3 °C 85 %RH, 108.2 °C vs. 105.5 °C WB).

As discussed in [31–33,38,51], environmental ageing can induce irreversible changes (such as interface crack/debonding, matrix pores/voids, and chemical composition changes), as well as reversible matrix swelling and hydrolysis. All these changes can cause T_g decrease. The similar value of T_g therefore implicitly indicates the same or similar material degradation induced by moisture absorption. Referring to the information illustrated in Figs. 3 and 4(a), as well as the T_g values for MD after drying given in Table 4, one can deduce that these irreversible changes (i.e. interface crack/debonding and matrix pores/voids) may be the same or similar for MD composite laminates after different environmental ageing. Detailed information related to the irreversible degradation could be provided via SEM examinations on the morphology of aged MD composite laminates in Section 4.1. In addition, the difference in T_g for MD composite laminates without drying treatment also indicates that more reversible matrix swelling and hydrolysis can occur at WB as compared to 85 %RH, due to more moisture

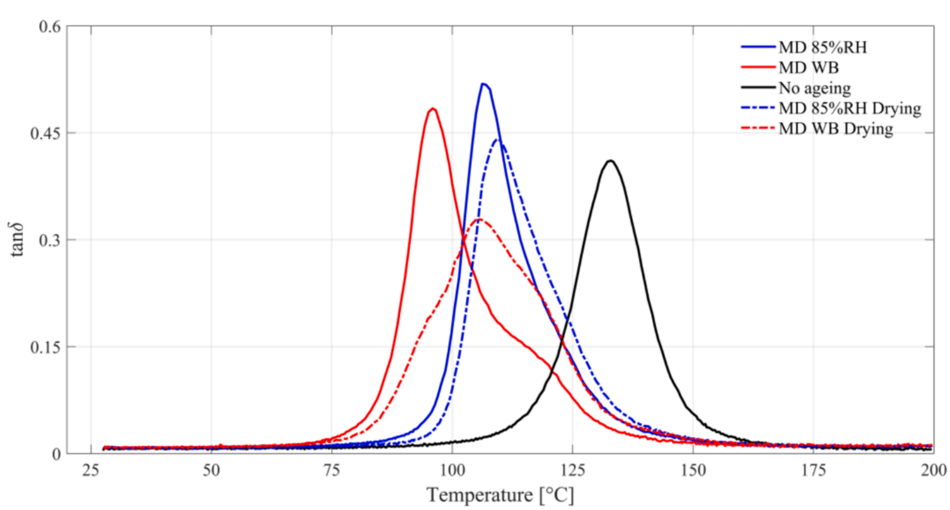

Fig. 5. DMAT results for MD composite laminates after different ageing.

Table 4
T_g for UD and MD at different ageing conditions.

	Ageing condition	T_g °C
MD composite laminates	n/a	133.0
	70 °C 85 %RH	106.3
	After drying	109.3
	70 °C WB	95.6
	After drying	105.5
UD composite laminates***	70 °C 85 %RH	107.4
	After drying	111.5
	70 °C WB	96.5
	After drying	108.2

*** Data of UD composite laminates are from [38,51].

absorption.

As a conclusion, the results given in Fig. 4 and Table 4 demonstrate that ageing severity has no effect on irreversible degradation, but causes difference in reversible matrix swelling and hydrolysis in composite laminates after different hygrothermal ageing. Layups have no influence on moisture absorption and material degradation at the same environmental ageing.

3.4. *Fatigue delamination analysis*

Both the modified Paris relation Eq.(1) and the two-parameter fatigue model Eq.(2) were employed to explore mode I intrinsic FDG around the crack front regardless of fibre bridging in MD composite laminates after different environmental ageing. According to these interpretations, a comparison was carried out (with fatigue delamination data of UD composite laminates after different environmental ageing [38,51]) to explore the effects of layups on mode I FDG after environmental ageing.

3.4.1. *Modified Paris interpretation*

As a prerequisite of using the modified Paris correlation Eq.(1) in fatigue data reduction, fatigue R-curve was determined via the specific test procedure proposed in [23,27,38,42,48,57]. Fig. 6 summarizes interlaminar resistance increase with fatigue delamination. It is clear that delamination resistance can increase significantly with crack growth. As discussed in [27,38,51,57], the presence of fibre bridging behind the crack front is the principal reason for this increase. This increase is independent on ageing severity and R-ratios in FDG of MD composite laminates, contributing to a single second-order polynomial curve-fitting as shown in Fig. 6. This means the development of fibre bridging in mode I fatigue delamination of MD composite laminates does not depend on either ageing severity nor stress ratio. For UD laminates [51], there is also no dependency on the ageing severity, but there is a strong dependence on R-ratio (see Fig. 6). A possible explanation for this may be related to crack closure. The stiffness of a UD DCB specimen is higher than that of a MD one with the same crack growth. Thus, for the

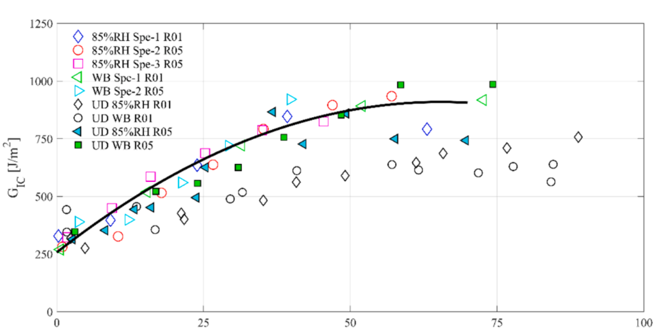

Fig. 6. Fatigue R-curves of MD and UD composite laminates after different ageing. Data of UD composite laminates are from [51].

same minimum force applied in a fatigue experiment, a larger value of displacement should be applied in MD specimen as compared to UD one. This increase in applied displacement can reduce crack closure in FDG with low stress ratio $R = 0.1$ of MD composite laminates.

Fig. 7 summarises mode I fatigue delamination interpretations in terms of da/dN against ΔG_{tip} for MD composite laminates after different ageing at different stress ratios $R = 0.1$ and 0.5, as well as the data reduction of UD composite laminates [51]. The use of this correlation Eq.(1) can make fatigue data with different amounts of fibre bridging converge into a narrow band region, contributing to a master resistance curve with moderate determination coefficient R^2 in determining FDG at a given R-ratio of MD composite laminates. The physical reason for the validity of using this relation in fatigue delamination determination has been given in [58]. The damage evolution around the crack front remains the same with fatigue delamination (i.e. fibre bridging development), physically making it reasonable to employ the *SERR* around the crack front (i.e. ΔG_{tip}) to represent the similarity in FDG characterization. Furthermore, a comparison on FDG between MD and UD composite laminates (see Fig. 7) demonstrate that there is the same fatigue delamination behaviour in composite laminates with different layups at a given R-ratio after the same environmental exposure, evidenced by the overlap of the delamination data in these graphs.

Data reduction illustrated in Fig. 7 enables a comparison on environmental ageing effects on mode I FDG in MD composite laminates, as shown in Fig. 8. Fatigue delamination after different environmental ageing at the same R-ratio remains the same, evidenced by the overlap of these results. As a result, a master resistance curve can be calibrated to describe FDG in MD composite laminates after different environmental ageing at the same R-ratio. The results illustrated in Fig. 8 also demonstrate that fatigue delamination growth rate can increase with stress ratio. The reason for this R-ratio dependence is attributed to the use of a similitude parameter that does not fully determine a fatigue cycle [9,19]. Thus the two-parameter fatigue model Eq.(2) will be adopted in the following section to have a generalized description of the FDG, as well as to provide extra information to explore hygrothermal ageing effects on mode I fatigue delamination in MD composite laminates. Furthermore, these interpretations can finally enable further comparison on layup effects on mode I FDG after different environmental ageing (incorporating with the UD fatigue data reported in [51]).

3.4.2. *Two-parameter fatigue law interpretation*

Fig. 9 summarizes all fatigue data interpreted via the two-parameter fatigue model Eq.(2) in terms of da/dN against ΔG_{eff}. The use of this model can well account for R-ratio effects, because of a full description of a fatigue cycle. Mode I fatigue delamination data from different environmental ageing at different R-ratios can converge into an overlapping band, demonstrating the same FDG behaviour regardless of ageing severity. As a result, a master resistance curve can be determined to represent mode I fatigue delamination of MD composite laminates after different hygrothermal ageing at various stress ratios.

According to the modified Paris law and the two-parameter fatigue law interpretations (see results illustrated in Fig. 8 and Fig. 9), one can make an important conclusion that the ageing severity indeed has negligible effects on mode I fatigue delamination of MD composite laminates. The physical reasons for this will be discussed in detail in Section 4 via fractographic analysis, incorporating with the FTIR and DMAT results provided in Sections 3.2 and 3.3.

3.4.3. *Comparison on fatigue delamination in UD and MD composite laminates*

Mode I fatigue delamination of UD composite laminates after different hygrothermal ageing have been investigated in the previous studies [38,51]. The fatigue delamination interpretation illustrated in Fig. 9 enables a comparison on mode I fatigue delamination between UD and MD composite laminates after different environmental ageing. Fig. 10 summarizes all these results in terms of da/dN against ΔG_{eff}. It is

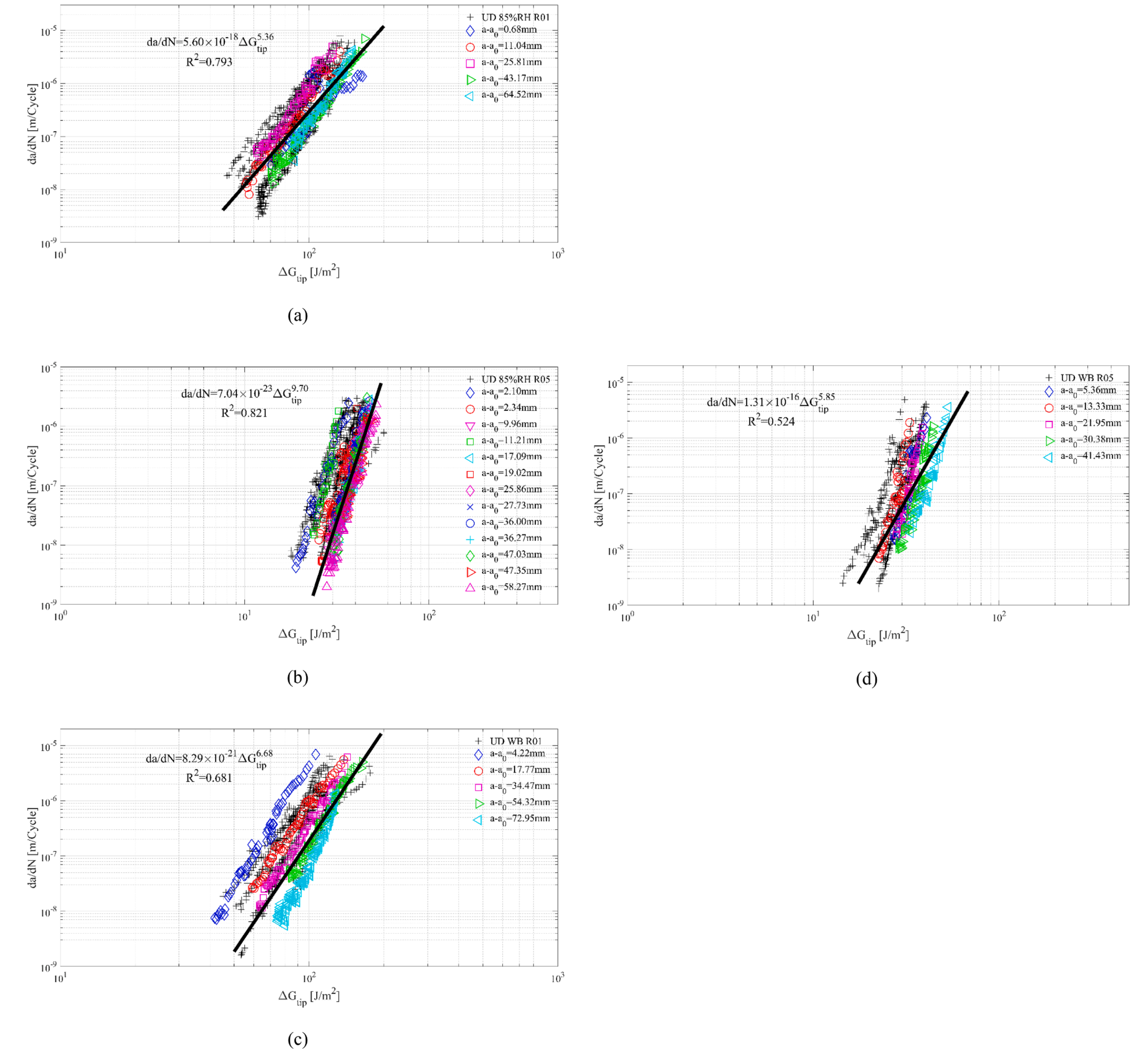

Fig. 7. Modified Paris law interpretation of mode I fatigue delamination. (a) and (c) for FDG in MD and UD composite laminates at $R = 0.1$ ageing at 85 % RH and WB respectively; (b) and (d) for FDG in MD and UD composite laminates at $R = 0.5$ ageing at 85 % RH and WB respectively. The trend lines represent MD data.

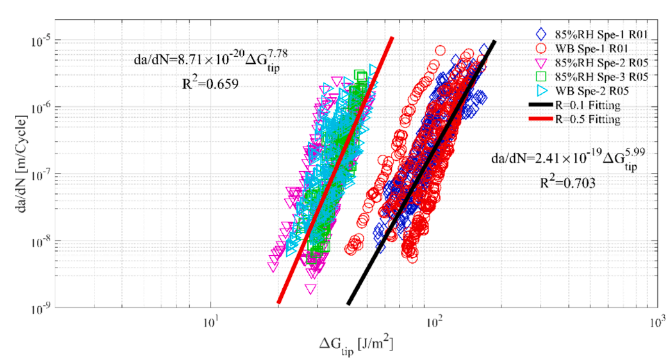

Fig. 8. *R*-ratio dependence of mode I fatigue delamination in MD composite laminates after different environmental ageing.

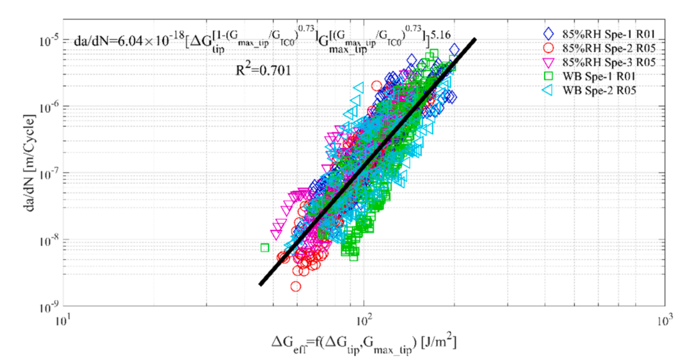

Fig. 9. Two-parameter fatigue model interpretation of mode I FDG of MD composite laminates after different environmental ageing at various *R*-ratios.

clear that fatigue delamination remains the same for composite laminates with different layups, as all data can overlap in the same narrow band. Curve-fitting were subsequently carried out to determine mode I FDG of UD and MD composite laminates. These fitted master resistance curves are almost identical, with the similar constants (6.04×10^{-18} vs. 5.27×10^{-18}) and exponents (5.16 vs. 5.23). It therefore can be concluded that layup has negligible effects on mode I fatigue delamination of composite laminates after different environmental ageing. The physical reasons for the same mode I fatigue delamination behaviour will be explored via fractographic examinations on both material morphology and delamination fracture surfaces in the following section.

According to the results illustrated in Fig. 6, fatigue R-curves show different *R*-ratio dependence for UD and MD composite laminates. One may ask questions that why this disappears in master resistance curves as shown in Fig. 10, and does this mean that master curves can mask the difference in fatigue delamination behaviour? As we mentioned, the use of the modified Paris relation Eq.(1) and the two-parameter fatigue law Eq.(2) indeed determine damage evolution concentrated around the crack front, regardless of fibre bridging. Thus, in physics, the same master resistance curve could be obtained if the damage mechanisms (as well as the material property) around the crack front are the same. Detailed information related to this will be given in the following SEM examinations on material morphology and fatigue fracture surfaces.

One may argue that the value of determination coefficient R^2 is not very high, but moderate. And it should be stressed that data scatter is an important issue frequently reported in fatigue study. Scholars indeed have paid attention and provided critical discussions related to scatter [59,60]. As discussed in these literature, the sources of scatter can be divided into intrinsic and extrinsic. The extrinsic scatter includes test set-up, operator experience, specimen preparation, cutting quality, variation in laminate thickness and so on. And the intrinsic scatter, related to inhomogeneous material morphology and process variability, can also have obvious effects on fatigue delamination data scatter. Particularly, fibre bridging can constitute as a source of intrinsic scatter [59]. To the authors' opinion, all above mentioned factors can have contribution to data scatter observed in fatigue delamination experiments as well as the corresponding data reduction. However, we only paid attention to hygrothermal aging effects on mode I fatigue delamination behaviour with fibre bridging in the present study. And data scatter is out the scope of this study.

4. Material morphology and fatigue delamination mechanisms

As illustrated in Figs. 8 and 9, while the ageing as such affects the FDG in UD and MD composite laminates, the change in the ageing severity has negligible effects on mode I fatigue delamination. The question arises as what are the physical reasons for this? Referring to the results illustrated in Figs. 7 and 10, one may also ask what are the physical reasons for the same mode I fatigue delamination in UD and MD

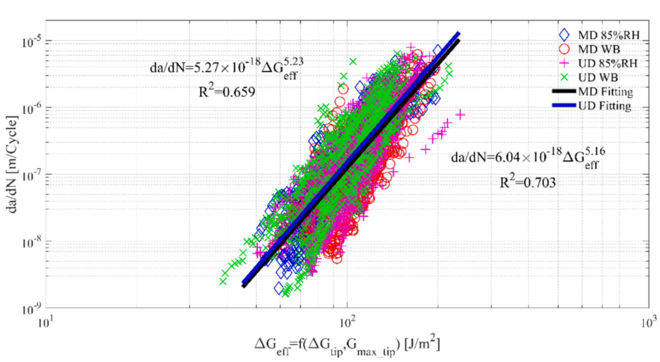

Fig. 10. Comparison on mode I fatigue delamination in UD and MD composite laminates after different hygrothermal ageing.

composite laminates. Fractographic examinations were therefore conducted to reveal these physical reasons: determine environmental ageing effects on material degradation and delamination mechanisms.

4.1. Material morphology of MD composite laminates

SEM observations were conducted on aged and un-aged MD composite laminates. Fig. 11 provides the microstructures of composite material M30SC/DT120 before and after different environmental ageing (SEM parameters: Magnification 10 kx, Detector E-T, Landing Energy 10 keV, Field of View (FoV) 25.1 μm, Beam Current (BM) 300 pA). It is clear that environmental ageing can have important influence on the appearance of MD composite laminates. However, the change of ageing severity has no obvious effects on the typical micro features identified in the material. For un-aged composite (see Fig. 11(a)), fibre/matrix interface is intact, and no obvious voids or manufacturing defects is observed in the matrix, indicating the high quality of the manufactured composite laminates used in this study. For different environmental exposure, both fibre/matrix debonding and matrix pores induced by water immersion can be identified as illustrated in Fig. 11(b)-(e). Particularly, interface debonding, evidenced by the white marking around the interface, distributes in the entire material, indicting degradation of fibre/matrix interface adhesion after environmental ageing. Pores are found in the matrix at some locations. All these degradations can promote crack initiation and propagation under cyclic loading. No obvious difference was identified on these microstructures for MD composite laminates after different environmental ageing. And the same moisture immersion induced features were also identified for UD composite laminates after different environmental ageing [38,51].

As discussed in Section 3.3, the magnitude of T_g could be treated as an indicator of composite material degradation after environmental ageing. Referring to the SEM observations (see Fig. 11) and FTIR analysis (see Fig. 4), one can deduce that the ageing severity has negligible effect on the irreversible degradation in MD composite laminates, i.e. the significance of fibre/matrix interface debonding and matrix pore generation induced by ageing generally remains the same. The fractographic examinations on UD [38,51] and MD composite laminates (see Fig. 11) shows that layup has no obvious effect on material degradation that is induced by water absorption, which is in line with the moisture absorption data (see Table 2), FTIR analysis (see Fig. 4) and the DMTA T_g (see Table 4). In the both ageing cases, local fibre debonding and inter-fibre matrix micro-pores appear, damage types which are not present in not-aged material. In the both cases, the intensity of these damage types is similar: debonding on the part of fibre surface (1/4 to 1/2 of the cross-section perimeter) and micro-pores with the size of few micrometres.

4.2. Fatigue delamination mechanisms in MD composite laminates

Figs. 12 and 13 summarize the SEM examinations for mode I fatigue delamination in MD composite laminates at different *R*-ratios after different environmental ageing (SEM parameters: Magnification 5 kx, Detector E-T, Landing Energy 10 keV, Field of View (FoV) 50.2 μm, Beam Current (BM) 300 pA). In general, no obvious difference on these micro features was observed on these surfaces with different ageing. Both dominant fibre prints, generated by fibre/matrix interface debonding, and matrix brittle failure, indicated by riverlines, scarps and hackles at some location, were observed on fatigue delamination surfaces, regardless of *R*-ratio or ageing severity. These typical features were also reported in fatigue delamination of MD composite laminates without ageing in our previous studies [27,61]. In addition to these features, both micro fibre/matrix interface debonding (something like wrinkle) and pores (in the resin matrix and around fibre/matrix interface) were identified on the fracture surfaces of aged MD composite laminates, which have not reported in mode I fatigue delamination of MD composite laminates without ageing [27,61]. The presence of these additional features are in line with the morphology results that

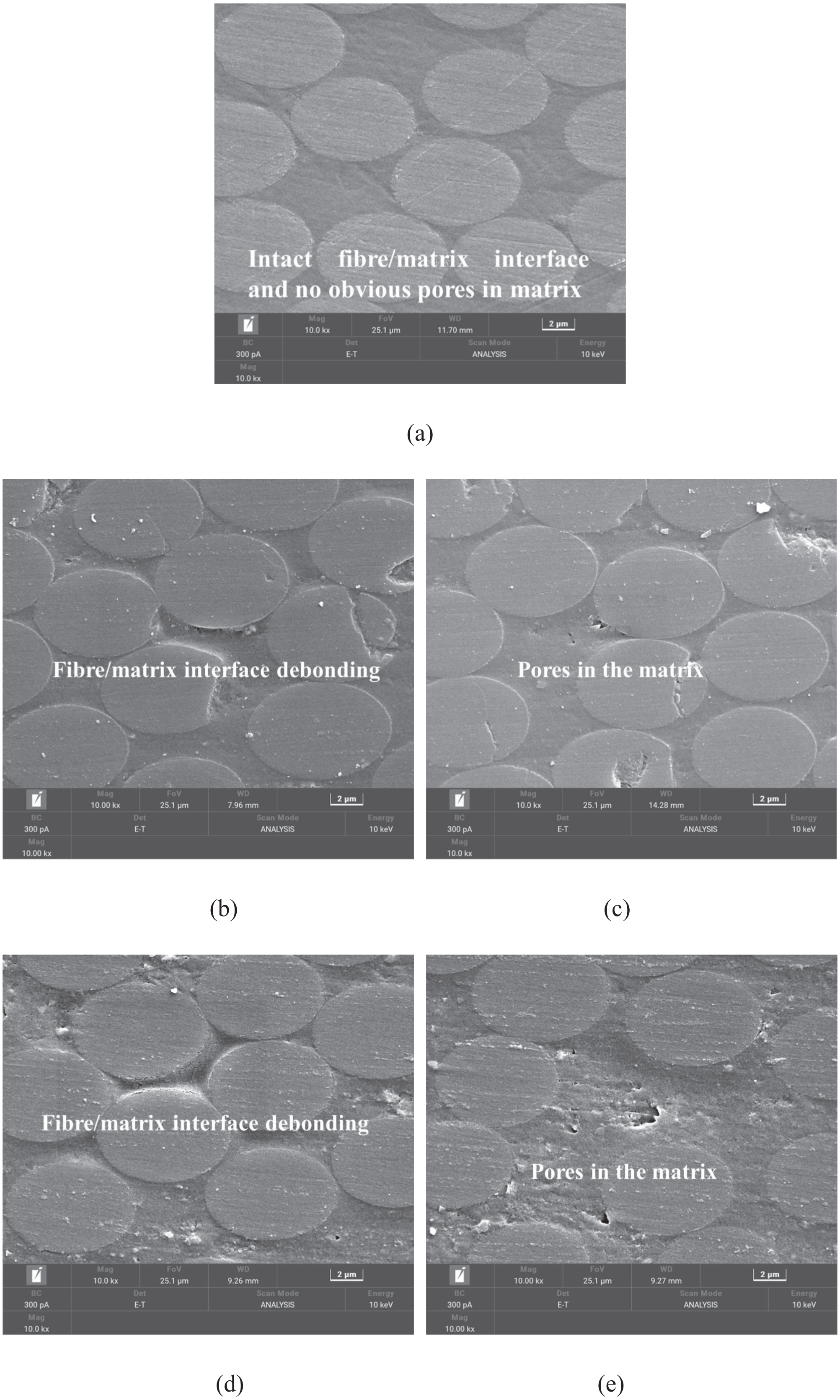

Fig. 11. The morphology of MD composite laminates with different environmental ageing: (a) No ageing; (b) and (c) for 70 °C 85%RH; (d) and (e) for 70 °C WB. White particles are contaminations.

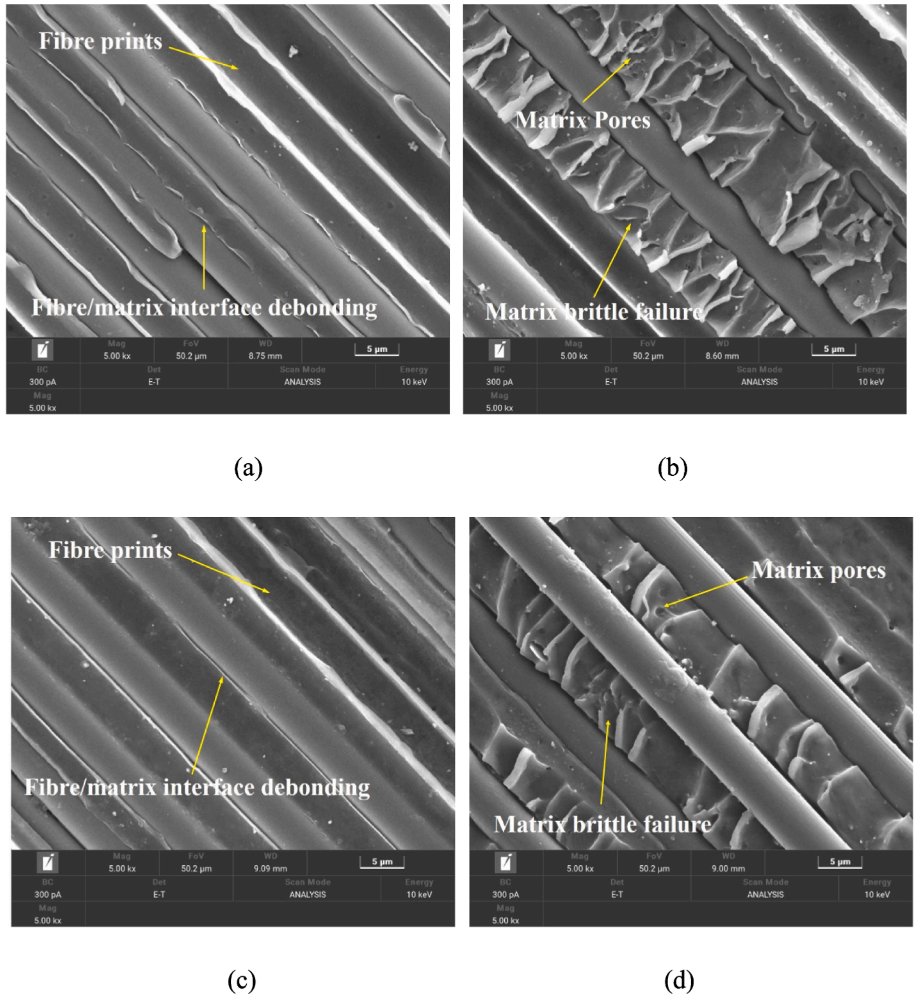

Fig. 12. Fractographic examinations on mode I fatigue fracture surfaces of MD composite laminates with 70 °C 85 %RH ageing: (a) and (b) for $R = 0.1$; (c) and (d) for $R = 0.5$.

illustrated in Fig. 11 (b)-(e), as both interface debonding and matrix pores are identified in environmentally aged MD composite laminates. And R-ratio has no obvious effect on mode I fatigue delamination mechanisms in MD composite laminates after different environmental ageing. The same damage mechanisms were also reported in mode I fatigue delamination of UD composite laminates after different ageing [38,51].

According to above discussions, it can be concluded that neither ageing severity nor layup has effect on material degradation or mode I fatigue delamination mechanisms. Particularly, environmental ageing can cause both fibre/matrix interface debonding and matrix pores, regardless of ageing severity or layup. Both dominant fibre prints and localized matrix brittle failure were identified on fatigue delamination surfaces, indicating the same damage mechanisms. These are the physical reasons for the same fatigue delamination behaviour observed in UD and MD composite laminates after different environmental ageing, see Figs. 7-10.

5. Concluding remarks

Mode I fatigue delamination in MD composite laminates at different R-ratios after different hygrothermal ageing (i.e. 70 °C 85 % RH and 70 °C WB) were investigated in the present study. It was found that ageing severity and layup has negligible influence on mode I FDG, according to fatigue data reduction via two Paris-type correlations.

The physical reasons for the same mode I FDG behaviour in UD and MD composite laminates after different environmental ageing were explored via FTIR, DMTA and SEM analysis. Particularly, it was found that there is no obvious irreversible chemical change, but reversible matrix swelling and hydrolysis reaction occurring in UD and MD composite laminates after different environmental ageing, according to the FTIR results. The SEM examinations on composite material morphology demonstrated that environmental ageing can cause irreversible interface debonding and matrix pores. Based on the DMTA T_g analysis, it was deduced that these irreversible degradation remains the same, regardless of ageing severity or layup. Fractographic analysis indicated that the damage mechanisms in fatigue delamination remain the same, regardless of ageing severity or layup. All these can finally contribute to the same mode I fatigue delamination in MD and UD composite laminates after different environmental ageing.

This study can provide solid evidence on the importance of using an appropriate similitude parameter in FDG characterization. The use of the modified Paris relation and the two-parameter fatigue model is not only valid in environmentally aged UD composite laminates, but also useful in MD composite laminates, contributing to data reduction agreeing well with the requirements of similitude principles.

The authors admit that we only conducted fatigue delamination investigations on MD composite laminates aged at two typical environmental conditions. One should keep in mind that composite materials or structures used in aeronautical engineering can endure even more

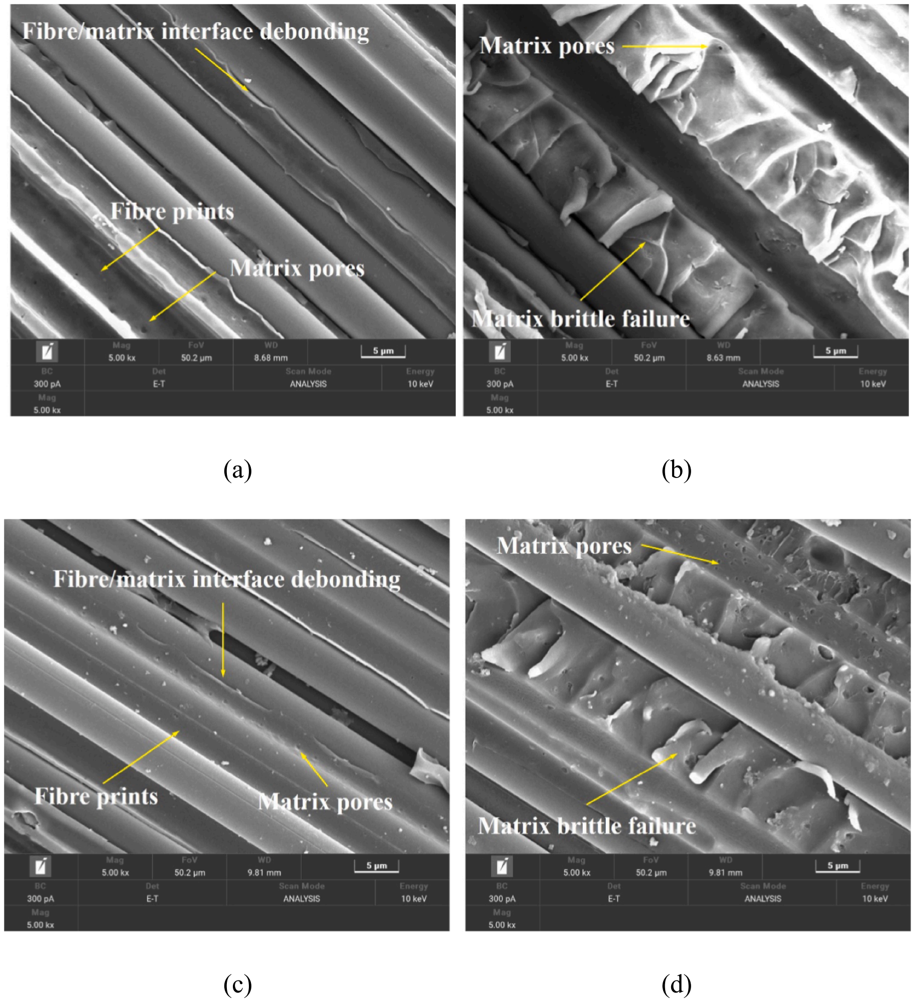

Fig. 13. Fractographic examinations on mode I fatigue fracture surfaces of MD composite laminates with 70 °C WB ageing: (a) and (b) for $R = 0.1$; (c) and (d) for $R = 0.5$.

complicated hygrothermal conditions during their long-term operation. Thus, more research work should be performed on composite laminates with even more complicated ageing conditions, such as a wide range of ageing temperatures and relative humidity, in order to have a full understanding on fatigue delamination behaviour of composite laminates after environmental ageing, which will be really meaningful for composite structure design and life evaluation.

CRediT authorship contribution statement

Liaojun Yao: Writing – review & editing, Writing – original draft, Visualization, Validation, Supervision, Software, Resources, Project administration, Methodology, Investigation, Funding acquisition, Formal analysis, Data curation, Conceptualization. **Zixian He:** Software, Formal analysis. **Yonglyu He:** Visualization, Validation, Software, Formal analysis. **Qifeng Jin:** Validation, Software, Methodology. **Stepan V. Lomov:** Writing – review & editing, Formal analysis, Data curation. **Rene C. Alderliesten:** Methodology, Data curation.

Declaration of competing interest

The authors declare that they have no known competing financial interests or personal relationships that could have appeared to influence the work reported in this paper.

Data availability

Data will be made available on request.

Acknowledgements

The authors gratefully acknowledge financial support from the National Natural Science Foundation of China with Grant No. 12272110 and 52303116, the Aeronautical Science Foundation of China with Grant No. 2022Z055077004, the National Key Laboratory of Strength and Structural Integrity Foundation with Grant No. ASSIKFJJ202302003, and the National Science Foundation of Hunan Province with Grant No. 2022JJ40548.

Appendix 1. . Prepreg properties

Tables A1, A2 show properties of the used matrix and prepreg according to the datasheet of Delta-Preg S.p.A., Toray Group (Italy).

Table A1
Properties of DT120 matrix.

Property	Value
Chemical nature	Epoxy Thermosetting Resin
Curing Temperature range	80 to 135 °C
Density of cured neat resin	1.22 g/cm^3
Dynamic viscosity	High, > 2000 Poise @ 60 °C, frequency 10 rad/sec.
T_g, cure cycle 90 min @ 120 °C	115—120

Table A2
Toray M30SC-DT120-200–36 UD Laminate, cured 90 min @ 120 °C, 6 Bar pressure.

Property	Value
Tensile Strength (0°) [MPa]	3010
Tensile Modulus (0°) [GPa]	145.0
Tensile Strength (90°) [MPa]	39
Tensile Modulus (90°) [GPa]	6.4
ILSS [MPa]	77.2
Areal density, g/m^2	200
M30SC fibre tensile modulus [GPa]	294

References

[1] Mueller EM, Starnes S, Strickland N, Kenny P, Williams C. The detection, inspection, and failure analysis of a composite wing skin defect on a tactical aircraft. Compos Struct 2016;145:186–93.

[2] Jones R, Kinloch AJ, Michopoulos JG, Brunner AJ, Phan N. Delamination growth in polymer-matrix fibre composites and the use of fracture mechanics data for material characterisation and life prediction. Compos Struct 2017;180:316–33.

[3] Federal Aviation Authority. Advisory circular AC 20-107B. Composite aircraft structure 2009.

[4] Brunner AJ, Murphy N, Pinter G. Development of a standardized procedure for the characterization of interlaminar delamination propagation in advanced composites under fatigue mode I loading conditions. Eng Fract Mech 2009;76:2678–89.

[5] Stelzer S, Brunner AJ, Arguelles A, Murphy N, Pinter G. Mode I delamination fatigue crack growth in unidirectional fiber reinforced composites: development of a standardized test procedure. Compos Sci Technol 2012;72:1102–7.

[6] Murri GB. Effect of data reduction and fiber-bridging on mode I delamination characterization of unidirectional composites. J Compos Mater 2014;48:2413–24.

[7] Stelzer S, Brunner AJ, Arguelles A, Murphy N, Cano GM, Pinter G. Mode I delamination fatigue crack growth in unidirectional fiber reinforced composites: results from ESIS TC4 round-robins. Eng Fract Mech 2014;116:92–107.

[8] Michel S, Murphy N, Kinloch AJ, Jones R. On cyclic-fatigue crack growth in carbon-fibre-reinforced epoxy-polymer composites. Polymers 2024;16:435.

[9] Pascoe JA, Alderliesten RC, Benedictus R. Methods for the prediction of fatigue delamination growth in composites and adhesive bonds- a critical review. Eng Fract Mech 2013;112-113:72–96.

[10] Bak BLV, Sarrado C, Turon A, Costa J. Delamination under fatigue loads in composite laminates: a review on the observed phenomenology and computational methods. Appl Mech Rev 2014;66:060803.

[11] Cano AJ, Salazar A, Rodriguez J. Evaluation of different crack driving forces for describing the fatigue crack growth behaviour of PET-G. Int J Fatigue 2018;107:27–32.

[12] Jensen SM, Bak BLV, Bender JJ, Lindgaard E. Transition-behaviours in fatigue-driven delamination of GFRP laminates following step changes in block amplitude loading. Int J Fatigue 2021;144:106045.

[13] Khan R, Alderliesten R, Benedictus R. Two-parameter model for delamination growth under mode I fatigue loading (Part B: Model development). Compos A Appl Sci Manuf 2014;65:201–10.

[14] Jones R, Molent L, Pitt S. Similitude and the Paris crack growth law. Int J Fatigue 2008;30:1873–80.

[15] Shahverdi M, Vassilopoulos AP, Keller T. A total fatigue life model for the prediction of the R-ratio effects on fatigue crack growth of adhesively-bonded pultruded GFRP DCB joints. Compos A Appl Sci Manuf 2012;43:1783–90.

[16] Yao LJ, Alderliesten RC, Benedictus R. Interpreting the stress ratio effect on delamination growth in composite laminates using the concept of fatigue fracture toughness. Compos A Appl Sci Manuf 2015;78:135–42.

[17] Jones R, Pitt S, Bunner AJ, Hui D. Application of the Hartman-Schijve equation to represent Mode I and Mode II fatigue delamination growth in composites. Compos Struct 2012;94:1343–51.

[18] Donough MJ, Gunnion AJ, Orifici AC, Wang CH. Scaling parameter for fatigue delamination growth in composites under varying load ratios. Compos Sci Technol 2015;120:39–48.

[19] Yao LJ, Cui H, Guo LC, Sun Y. A novel total fatigue life model for delamination growth in composite laminates under generic loading. Compos Struct 2021;258:113402.

[20] Sebaey TA, Blanco N, Costa J, Lopes CS. Characterization of crack propagation in mode I delamination of multidirectional CFRP laminates. Compos Sci Technol 2012;72:1251–6.

[21] Farmand-Ashtiani E, Alanis D, Cugnoni J, Botsis J. Delamination in cross-ply laminates: Identification of traction-separation relations and cohesive zone modeling. Compos Sci Technol 2015;119:85–92.

[22] Gong Y, Chen XJ, Li WC, Zhao LB, Tao J, Zhang JY, et al. Delamination in carbon fiber epoxy DCB laminates with different stacking sequence: R-curve behavior and bridging traction-separation relation. Compos Struct 2021;113605.

[23] Yao LJ, Sun Y, Alderliesten RC, Benedictus R, Zhao MY. Fibre bridging effect on the Paris relation for mode I fatigue delamination growth in composites with consideration of interface configuration. Compos Struct 2017;159:471–8.

[24] van der Panne M, Pascoe JA. Fatigue delamination growth – Is UD testing enough? Procedia Struct Integrity 2022;42:449–56.

[25] Peng L, Zhang JY, Zhao LB, Bao R, Yang HQ, Fei BJ. Mode I delamination growth of multidirectional composite laminates under fatigue loading. J Compos Mater 2010;45:1077–90.

[26] Peng L, Xu JF, Zhang JY, Zhao LB. Mixed mode delamination growth of multidirectional composite laminates under fatigue loading. Eng Fract Mech 2012;96:676–86.

[27] Yao LJ, Cui H, Sun Y, Guo LC, Chen XM, Zhao MY, et al. Fibre-bridged fatigue delamination in multidirectional composite laminates. Compos A Appl Sci Manuf 2018;115:175–86.

[28] Ishbir C, Banks-Sills L, Fourman V, Eliasi R. Delamination propagation in a multi-directional woven composite DCB specimen subjected to fatigue loading. Compos B Eng 2014;66:180–9.

[29] Banks-Sills L, Simon I, Chocron T. Muliti-directional composite laminates: fatigue delamination propagation in mode I - a comparison. Int J Fract 2019;219:175–85.

[30] Zhao LB, Gong Y, Zhang JY, Wang YN, Lu ZZ, Peng L, et al. A novel interpretation of fatigue delamination growth behavior in CFRP multidirectional laminates. Compos Sci Technol 2016;133:79–88.

[31] Khan LA, Mahmood AH, Syed AS, Khan ZM, Day RJ. Effect of hygrothermal conditioning on the fracture toughness of carbon/epoxy composites cured in autoclave/Quickstep. J Reinf Plast Compos 2013;32:1165–76.

[32] Wang Z, Xian G, Zhao X. Effects of hydrothermal aging on carbon fibre/epoxy composites with different interfacial bonding strength. Constr Build Mater 2018;161:634–48.

[33] Niu YF, Yan Y, Yao JW. Hygrothermal aging mechanism of carbon fiber/epoxy resin composites based on quantitative characterization of interface structure. Polym Test 2021;94:107019.

[34] Abanilla MA, Karbhari VM, Li Y. Interlaminar and intralaminar durability characterization of wet layup carbon/epoxy used in external strengthening. Compos B Eng 2006;37:650–61.

[35] Wang S, Akbolat MC, Katnam KB, et al. The effect of hygrothermal ageing on the delamination of Carbon/epoxy laminates with Core-shell rubber nanoparticle and Micro-fibre thermoplastic veil toughening. Compos Part A: Appl Sci Tech 2023;171:107576.

[36] Alessi S, Pitarresi G, Spadaro G. Effect of hydrothermal ageing on the thermal and delamination fracture behaviour of CFRP composites. Compos B Eng 2014;67:145–53.

[37] Tual N, Carrere N, Davies P, Bonnemains T, Lolive E. Characterization of sea water ageing effects on mechanical properties of carbon/epoxy composites for tidal turbine blades. Compos A Appl Sci Manuf 2015;78:380–9.
[38] Yao LJ, Wang JX, He YL, Zhao XH, Chen XM, Liu JR, et al. Hygrothermal effects on fatigue delamination behavior in composite laminates. Compos Struct 2024;330:117830.
[39] Nakai Y, Hiwa C. Effects of loading frequency and environment on delamination fatigue crack growth of CFRP. Int J Fatigue 2002;24:161–70.
[40] van den Akker BPH, Donadon MV, Loendersloot R, et al. The influence of hygrothermal ageing on the fatigue behavior and residual strength of post-buckled co-bonded stiffened panels subjected to compression loading. Compos B Eng 2020;194:108023.
[41] LaPlante G, Landry B. The effect of hygrothermal aging on mode I fatigue delamination growth in a carbon/epoxy composite. J Adv Mater 2011;43:79–86.
[42] Yao LJ, Alderliesten RC, Jones R, Kinloch AJ. Delamination fatigue growth in polymer-matrix composites: a methodology for determining the design and lifing allowables. Compos Struct 2018;196:8–20.
[43] Mamalis D, Floreani C, Bradaigh CMO. Influence of hygrothermal ageing on the mechanical properties of unidirectional carbon fibre reinforced powder epoxy composites. Compos B Eng 2021;225:109281.
[44] Sebaey TA, Blanco N, Lopes CS, Costa J. Numerical investigation to prevent crack jumping in Double Cantilever Beam tests of multidirectional composite laminates. Compos Sci Technol 2011;71:1587–92.
[45] ASTM D5528-01 Standard test method for Mode I interlaminar fracture toughness of unidirectional fiber-reinforced polymer matrix composites. 2001.
[46] ASTM D5229/5229M-20. Standard test method for moisture absorption properties and equilibrium conditioning of polymer matrix composite materials. 2020.
[47] Ramirez FMG, Garpelli FP, et al. Hygrothermal effects on the fatigue delamination growth onset in interlayer toughened CFRP joints. Int J Fatigue 2020;138:105729.
[48] Yao LJ, Chuai MY, Lyu ZM, Chen XM, Guo LC, Alderliesten RC. A proposal for similitude in characterizing fatigue delamination behavior with fibre bridging of carbon-fibre reinforced polymer composites. Eng Fract Mech 2024;295:109756.
[49] Lahuerta F, Westphal T, Nijssen RPL, van der Meer FP, Sluys LJ. Measuring the delamination length in static and fatigue mode I tests using video image processing. Compos B Eng 2014;63:1–7.
[50] ASTM E647-00. Standard test method for measurement of fatigue crack growth rates. 2000.
[51] Yao LJ, Wei JC, He ZX, He YL, Lomov SV, Alderliesten RC. Does hygrothermal degradation of mode I fatigue delamination resistance in carbon fibre reinforced polymer laminates depend on the ageing conditions? Compos Struct 2024;342:118240.
[52] Stevens GC. Cure kinetics of a high epoxide/hydroxyl group-ratio bisphenol a epoxy resin - anhydride system by infrared absorption spectroscopy. J Appl Polym Sci 1981;26:4279–97.
[53] Lin YC, Chen X, Zhang HJ, Wang ZP. Effects of hygrothermal aging on epoxy-based anisotropic conductive film. Mater Lett 2006;60:2958–63.
[54] Wang YL, Meng ZP, Zhu WX, Wan BL, Han BG, Cai GC, et al. Hygrothermal aging behavior and aging mechanism of carbon nanofibers/epoxy composites. Constr Build Mater 2021;294:123538.
[55] Gao JC, Li X, Wei JH, Zhang YH, Wang JH, Ding AX. Hygrothermal behavior of carbon fiber fabric reinforced vinylester resin composite structures. Appl Compos Mater 2024.
[56] Jojibabu P, Ram GDJ, Deshpande AP, Bakshi SR. Effect of carbon nano-filler addition on the degradation of epoxy adhesive joints subjected to hygrothermal aging. Polym Degrad Stab 2017;140:84–94.
[57] Yao LJ, Chuai MY, Li HY, Chen XM, Quan D, Alderliesten RC, et al. Temperature effects on fatigue delamination behavior in thermoset composite laminates. Eng Fract Mech 2024;295:109799.
[58] Yao LJ, Cui H, Alderliesten RC, Sun Y, Guo LC. Thickness effects on fibre-bridged fatigue delamination growth in composites. Compos A Appl Sci Manuf 2018;110:21–8.
[59] Alderliesten RC, Brunner AJ, Pascoe JA. Cyclic fatigue fracture of composites: what has testing revealed about the physics of processes so far? Eng Fract Mech 2018;203:186–96.
[60] Brunner AJ. Fracture mechanics testing of fiber-reinforced polymer composites: the effects of the "human factor" on repeatability and reproducibility of test data. Eng Fract Mech 2022;264:108340.
[61] Yao LJ, Sun Y, Guo LC, Lyu XQ, Zhao MY, Jia LY, et al. Mode I fatigue delamination growth with fibre bridging in multidirectional composite laminates. Eng Fract Mech 2018;189:221–31.